Creep-fatigue crack growth behavior of Sn-37Pb and Sn-3.0Ag-0.5Cu solders at room and elevated temperatures

K. Fakpan[1], S. Inoue[2], K. Nagata[3], Y. Otsuka[4], Y. Mutoh[4,*]

[1] Graduate student, Dept. of Materials Science, Nagaoka University of Technology, Nagaoka-shi, Niigata, Japan, 940-2188
[2] Graduate student, Dept. of Mechanical Engineering, Nagaoka University of Technology, Nagaoka-shi, Niigata, Japan, 940-2188
[3] Toshiba Corporation, Toshiba-cho, Fuchu-shi, Tokyo, Japan, 183-8511
[4,*]*Dept. of System Safety, Nagaoka University of Technology, Nagaoka-shi, Niigata, Japan, 940-2188
*Corresponding Author: mutoh@mech.nagaokaut.ac.jp, Tel: 81 258 47 9735, Fax: 81 258 47 9770

Abstract

Fatigue crack growth tests of Sn-37Pb and Sn-3.0Ag-0.5Cu solders were conducted under frequencies from 10 to 0.1 Hz and a stress ratio of 0.1 at room temperature and 70°C. J-integral range (ΔJ) and modified J-integral (C^*) were used to discuss about cycle-dependent and time-dependent crack growth behavior. The experimental results showed that crack growth behavior of both the solders were predominantly time-dependent at lower frequency and higher temperature, while it was predominantly cycle-dependent at higher frequency and lower temperature. Furthermore, from the fracture surface observations of both the solders, it was found that as the frequency decreased and/or the temperature increased, the fracture surface appearance changed from transgranular to intergranular manner for both the solders.

Keywords: Lead-contained solder, Lead-free solder, Fatigue crack growth, Creep crack growth, Frequency, Temperature

1. Introduction

Generally solder joints were subject to cyclic loading during processing and service due to the mismatch of thermal expansion coefficient between components as well as mechanical vibration [1]. Since the strength of solder is lower than other components, most of cyclic stress and strain are generated in the solder [2]. Moreover under usual operating conditions, the temperature of solder joints in the electronic packages ranges between 25°C and 100°C, which corresponds to quite a high homologous temperature [3]. Therefore, the damage from fatigue, creep and their combination may take place in the solder during their operation.

Fatigue damage consists of crack nucleation and growth. However, since crack nucleation of solder joints is generally early, crack growth process is dominant for fatigue life of solder joint [4, 5]. Thus the capability to predict the crack growth behavior is vital for lift estimation of the solder joint. For understanding

crack growth behavior of solders, Zhao et al. [6] conducted fatigue crack growth test of Sn-3.5Ag at room temperature under frequencies from 0.1 to 10 Hz with stress ratio of 0.1 to 0.7. They reported that fatigue crack growth behavior of Sn-3.5Ag changed from cycle-dependent to time dependent when stress ratio increased and frequency decreased. In case of Sn-37Pb and Sn-3.0Ag-0.5Cu solders, Zhao et al. [7] also reported that the fatigue crack growth behavior was predominantly time-dependent for the frequencies of 0.1 Hz under stress ratio of 0.1 and 10 Hz under stress ratio of 0.7 at room temperature. Nevertheless, more work is needed to understand the details of crack growth behavior of Sn-37Pb and Sn-3.0Ag-0.5Cu solders, especially at elevated temperature.

In the present work, effects of temperature and frequency on creep-fatigue crack growth behavior of Sn-37Pb and Sn-3Ag-0.5Cu solders were investigated. The time dependency of fatigue crack growth (FCG) process was investigated by decreasing the cyclic frequency from 10 Hz to 0.1 Hz and increasing temperature from room temperature to 70°C. In addition the creep crack growth (CCG) tests were also conducted for comparison.

2. Experimental procedure

2.1 Materials

The solders used are as-cast Sn-37Pb and Sn-3.0Ag-0.5Cu alloys. Chemical composition of the solders used is shown in Table 1. Mechanical properties of the solders used are shown in Table 2. The microstructure of Sn-37Pb solder is composed of β-Sn phase (dark) and Pb-rich phase (light) as seen from Fig. 1a. For the Sn-3.0Ag-0.5Cu solder, the microstructure is composed of dendritic β-Sn phase (dark) and eutectic network of dispersed Ag_3Sn (light) and Cu_6Sn_5 intermetallic compounds within the β-Sn phase as seen from Fig. 1b. However, Cu_6Sn_5 intermetallic compound could not be found from Fig. 1b due to the less amount of copper content.

Table. 1 Chemical composition of the Sn-37Pb and Sn-3.0Ag-0.5Cu solders. (mass%)

Solder	Ag	Cu	Pb	Sn
Sn-3.0Ag-0.5Cu	3.0	0.51	0.029	Bal.
Sn-37Pb	-	0.0016	36.68	Bal.

Table. 2 Mechanical properties of the Sn-37Pb and Sn-3.0Ag-0.5Cu solders.

Solder	Young's modulus (GPa)	Yield strength (MPa)	Tensile strength (MPa)
Sn-3.0Ag-0.5Cu	54	25.3	50.6
Sn-37Pb	30.2	18.1	39.7

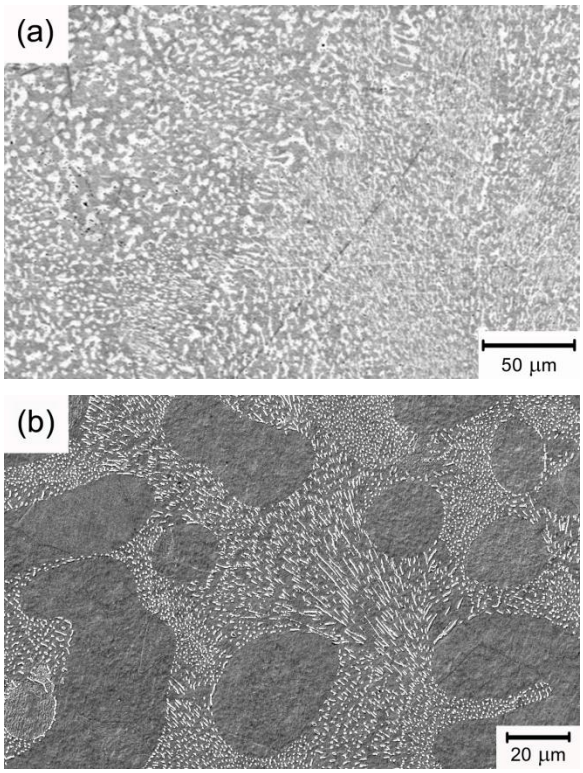

Fig.1. Microstructure of (a) as-cast Sn-37Pb alloy and (b) as-cast Sn-3.0Ag-0.5Cu alloy.

2.2 Crack growth experiments

The center cracked tension (CCT) plate specimen with 20 mm in gauge length, 20 mm in width and 2 mm in thickness was used for the crack growth tests. The specimens were cut by using an NC machine and a center notch was introduced by an EDM wire cut machine. After the specimens were machined, their gauge section was polished by using 0.25 μm diamond paste and then annealed at 154°C for 1 hr for homogenizing microstructure and reducing residual stress according to the Low Cycle Fatigue Standard for Solder Testing, Japan Society of Materials Science (JSMS) [8]. The crack growth tests were conducted on a servo-hydraulic fatigue machine with 1 kN capacity of load-cell. Crack length was measured by using a traveling microscope with an accuracy of 10 μm. In order to increase the specimen temperature during crack growth tests, two resistance-type heating elements were attached at upper and lower parts of specimen. The fluctuation of test temperature in the gauge part was maintained within a range of ±1°C. All crack growth tests were conducted in laboratory air at temperatures of 21°C (room temperature) and 70°C. Fatigue crack growth tests were conducted by using sinusoidal waveform of loading with a stress ratio of 0.1 at frequencies of 10, 1 and 0.1 Hz. Creep crack growth tests were also conducted under constant load. Before the tests, all specimens were introduced a fatigue precrack with length of 0.5 mm at each side of notch root. The final ΔK used for precracking was equal to the initial ΔK used for fatigue and creep crack growth tests.

2.3 Fracture mechanics parameter

Since the solders are low yield strength materials, a large plastic zone will be formed ahead of crack tip during fatigue crack growth tests. J-integral range (ΔJ) is an effective parameter for the large scale yielding condition. Therefore, ΔJ was evaluated for discussing FCG behavior. For center cracked tension specimen, ΔJ can be evaluated by the following equation [9, 10].

$$\Delta J = \frac{(\Delta K)^2}{E} + \frac{S_p}{B(W-2a)} \quad (1)$$

where ΔK is the stress intensity factor range, E Young's modulus, S_p the area beneath the load versus displacement curve, B the specimen thickness, W the specimen width and a the half crack length.

C^* parameter was used for discussing crack growth behavior of solder in creep regime [11]. For CCT specimen, C^* parameter was evaluated by the following equation [12].

$$C^* = \frac{n-1}{n+1} \frac{P}{B(W-2a)} \dot{\delta}_{COD} \quad (2)$$

where n is the creep stress exponent, P the applied load and $\dot{\delta}_{COD}$ the crack opening displacement rate. The creep stress exponent for Sn-37Pb and Sn-3.0Ag-0.5Cu solders were obtained by creep test as show in Table 3.

Table. 3 Creep stress exponent for Sn-37Pb and Sn-3.0Ag-0.5Cu solders

Solder	*n* value	
	21°C	70°C
Sn-37Pb	4.6	3.34
Sn-3.0Ag-0.5Cu	5.05	4.1

3. Results and discussions

The crack growth rates were evaluated as a function of J-integral range (ΔJ) and C^* by using secant method according to the ASTM standard E649 [13].

3.1 J-integral range

Figure 3 shows relationship between cycle-dependent crack growth rate (*da/dN*) and ΔJ for Sn-37Pb and Sn-3.0Ag-0.5Cu solders tested under various frequencies at room temperature and 70°C. As seen from the figure, there are five groups: the first group is those tested at room temperature under f = 10 and 1 Hz for both the solders, the second is those tested at 70°C under f = 10 Hz for both the solders, the third is that tested at room temperature under f = 0.1 Hz for Sn-37Pb solder, the fourth is that tested at room temperature under f = 0.1 Hz for Sn-3.0Ag-0.5Cu solder, and the fifth is those tested at 70°C under f = 1 and 0.1 Hz for both the solders. The first and second groups indicated similar slope, while the crack growth rate was higher at 70°C compared to that at room temperature. The other three groups showed similar slope, which were steeper than those for the first and second groups. The crack growth rate of the fifth group tested at 70°C was higher than those tested at room temperature. As mentioned above, the sloped of the crack growth curves for frequencies of 0.1 and 1 Hz at 70°C and for 0.1 Hz at room temperature were steeper than those for 10 Hz at 70°C and for 10 and 1 Hz at room temperature. This may suggest significant creep effect, that is time-dependent crack growth, at lower frequency and higher temperature. In the next section, time-dependent crack growth behavior has been discussed.

3.2 Modified J-integral, C^*

Relationship between time-dependent crack growth rate (*da/dt*) and C^* parameter for Sn-37Pb and Sn-3.0Ag-0.5Cu solders tested under various frequencies at room temperature and 70°C is shown in Fig. 4. Creep crack growth data at room temperature and 70°C for both the solders are also indicated in the figure. As seen from the figure, creep crack growth resistance of the Sn-3.0Ag-0.5Cu solder was higher than that of the Sn-37Pb solder. The crack growth data for 0.1 Hz at room temperature and for 0.1 and 1 Hz at 70°C were laid in the scatter bands of creep crack growth for the Sn-37Pb and Sn-3.0Ag-0.5Cu solders. On the other hand, crack growth data for 1 and 10 Hz at room temperature and 10 Hz at 70°C were placed upper the creep crack growth curves, which would be induced by acceleration of crack growth rate due to cyclic fatigue effect.

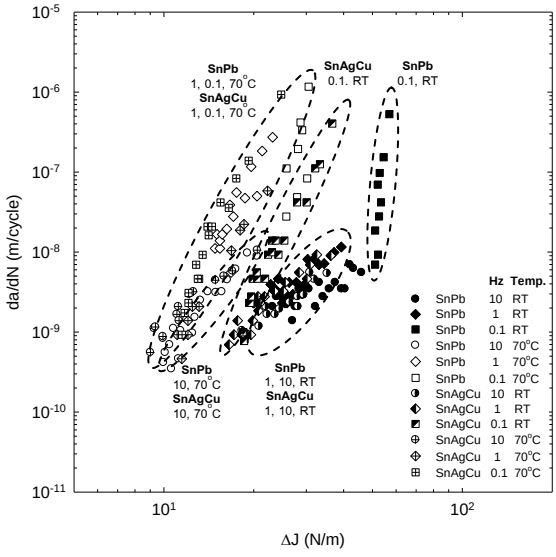

Fig. 3 Relationship between *da/dN* and ΔJ for Sn-37Pb and Sn-3.0Ag-0.5Cu solders.

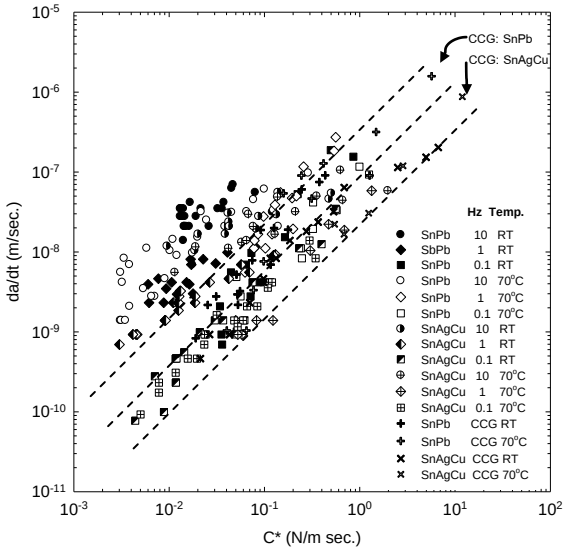

Fig. 4 Relationship between *da/dt* and *C** for Sn-37Pb and Sn-3.0Ag-0.5Cu solders.

3.3 Fractography

After the crack growth tests at room temperature and 70°C, the failed specimens were cleaned in an ultrasonic cleaner for 30 minutes with acetone and subsequently their fracture surfaces were observed using a scanning electron microscope. The fracture surfaces of Sn-37Pb and Sn-3.0Ag-0.5Cu solder tested under cycle-dependent condition (10 and 1 Hz at room temperature and 10 Hz at 70°C) were predominantly transgranular fracture mode. For example, the typical transgranular fracture for Sn-37Pb solder is showed in Fig. 5.

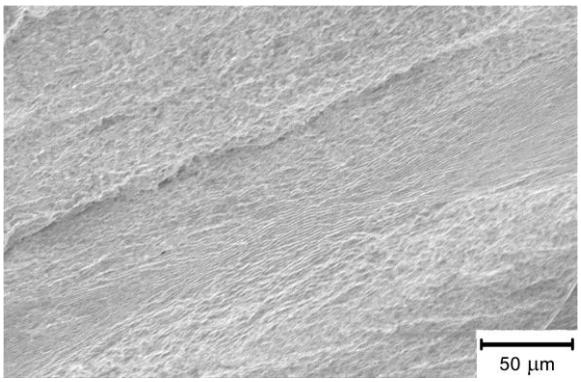

Fig. 5 Typical transgranular fracture surface for Sn-37Pb solder tested under a frequency of 10 Hz at room temperature.

For transgranular fracute surface of Sn-3.0Ag-0.5Cu solder, the micro-crack was often observed in the eutectic band as well as β–Sn /eutectic interface as shown in Fig. 6.

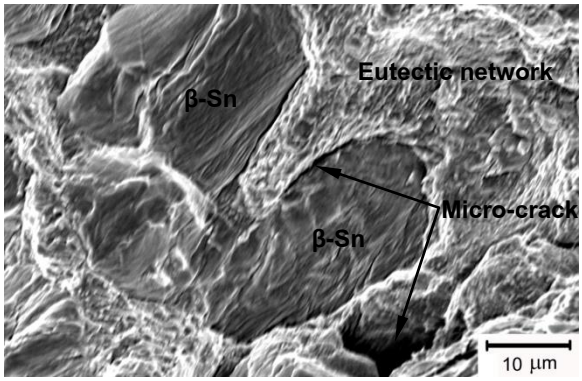

Fig. 6 Typical transgranular fracture surface for Sn-3.0Ag-0.5Cu solder tested under a frequency of 10 Hz at room temperature.

Whereas the fracture surfaces for Sn-37Pb tested under time-dependent condition (0.1 Hz at room temperature and 1 and 0.1 Hz at 70°C as well as CCG tests) were found predominantly intergranular. For example, Fig. 7a and 7b show fracture surfaces of CCG and FCG specimens at low magnification. As seen from the figure, their fracture surfaces consist of three region including fatigue precrack, crack growth region and overload region. At high magnification in area A of the crack growth region of Fig. 7b, small dimples on grain facets could be seen more clearly as shown in Fig. 8.

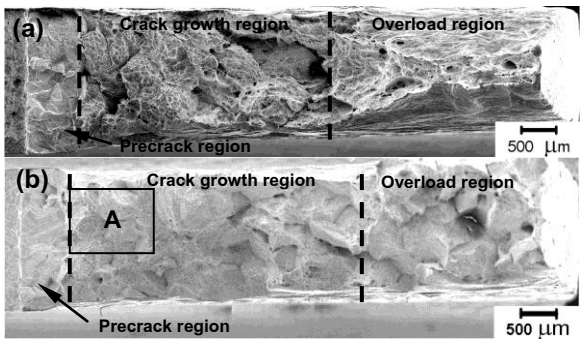

Fig. 7 Fracture surface at low magnification of Sn-37Pb solder for (a) CCG and (b) FCG tested under a frequency of 0.1 Hz at 70°C

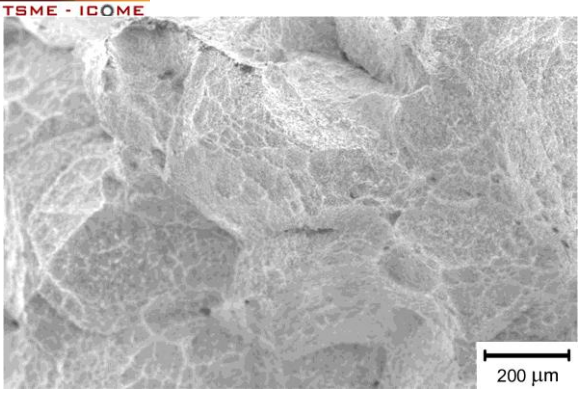

Fig. 8 Typical fracture surface of intergranular for Sn-37Pb solder tested under a frequency of 0.1 Hz at 70°C

For Sn-3.0Ag-0.5Cu solder, Fig. 9a and 9b show fractures surface at low magnification of CCG and FCG specimens tested under frequency of 0.1 Hz at 70°C respectively. As seen from the figure, the crack growth regions of both CCG and FCG specimens show ductile fracture and then significant necking was observed in the final stage of fracture. At high magnification as shown in Fig. 10, large ductile dimples could be seen clearly in area B of FCG specimen. From the cross-section observation as shown in Fig. 11, it was confirmed that the fracture surface of Sn-3.0Ag-0.5Cu solder tested under time-dependent condition was predominantly intergranular.

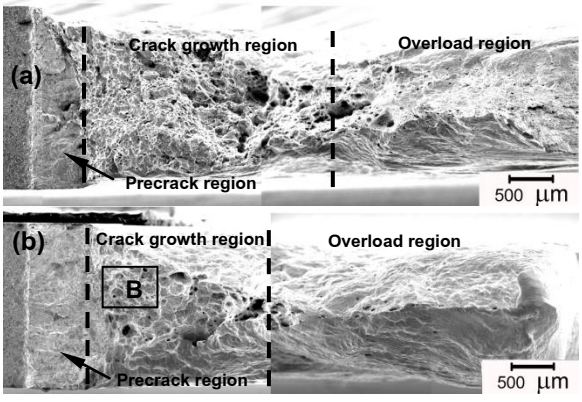

Fig. 9 Fracture surface at low magnification of Sn-3.0Ag-0.5Cu for (a) CCG and (b) FCG tested under a frequency of 0.1 Hz at 70°C.

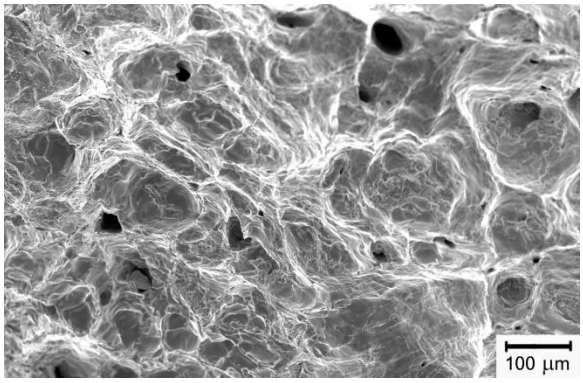

Fig 10. Ductile dimple fracture surface of Sn-3.0Ag-0.5Cu solder tested under a frequency of 0.1 Hz at 70°C.

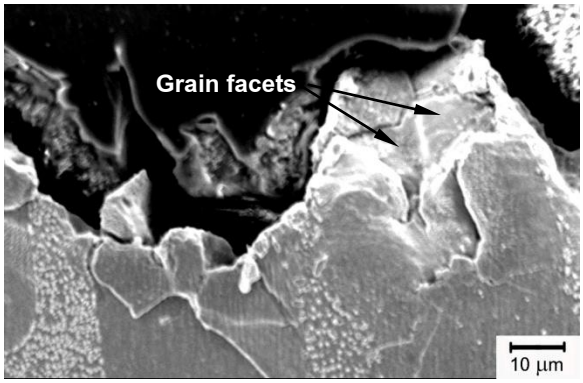

Fig. 11 The cross-sections through the fractured surface of Sn-3.0Ag-0.5Cu solder tested under a frequency of 0.1 Hz at 70°C.

3.4 Recrystallization

Room temperature and 70°C are higher than homologous temperatures of the solders. Recrystallization of Sn-5Pb, Sn-37Pb solders [6] and SnAgCu solder joint [15] during fatigue and creep tests has been reported. In the present investigation, small grains of Sn-3.0Ag-0.5Cu solder were often observed in β-Sn phase in the region near the fracture surface, as shown in Fig. 12. It is suggested that a large plastic deformation around the crack tip is the driving force for small grain formation due to the high stacking fault energy of tin.

3.5 Cycle- and time-dependent transition of crack growth behavior

According to the foregoing results and discussion, Fig.13 shows a summary of fatigue crack growth behavior of Sn-37Pb and Sn-3.0Ag-0.5Cu solders tested under frequencies from 10 Hz to 0.1 Hz with a stress ratio of 0.1 at room temperature and 70°C. The fatigue crack growth behavior of both the solders was a predominantly cycle-dependent behavior with transgranular fracture manner at high frequency and low homologous temperature, whereas the fatigue crack growth behavior was changed to time-dependent with intergranular fracture manner for both the solders under the low frequency and high homologous temperature. The transition between cycle-dependent and time-dependent for the present solders is shown in the figure as a broken line. When the stress ratio becomes high, the transition may move to higher frequency and lower temperature side according to the result reported [7], which is also shown in Fig.13.

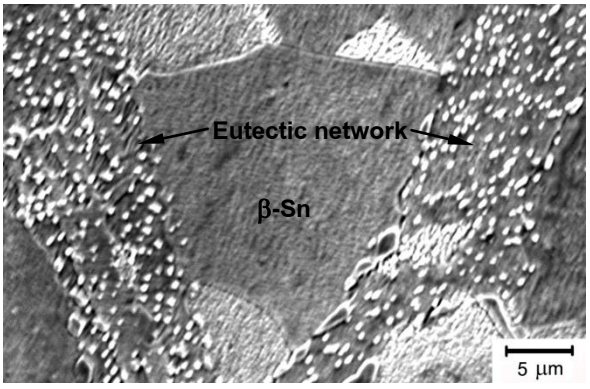

Fig. 12 Microstructure near the fracture surface of Sn-3.0Ag-0.5Cu solder tested under a frequency of 10 Hz at room temperature

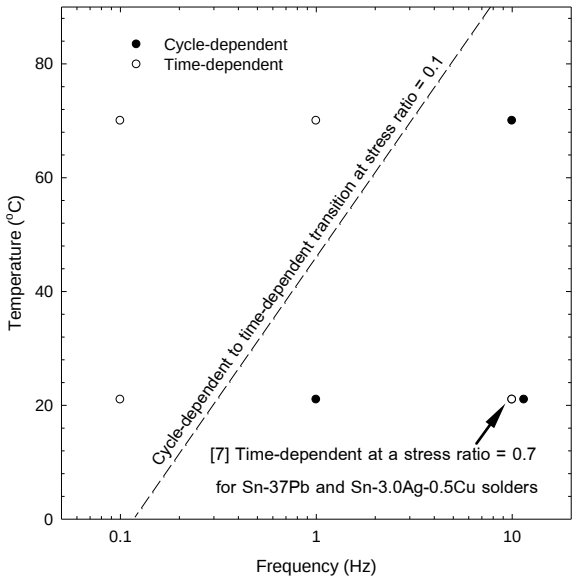

Fig 13. Summary of crack growth behavior of Sn-37Pb and Sn-3.0Ag-0.5Cu solders.

4. Conclusion

1. The fatigue crack growth behavior of Sn-37Pb and Sn-3.0Ag-0.5Cu solders tested under frequencies of 10 and 1 Hz at room temperature and 10 Hz at 70°C were predominantly cycle-dependent with transgranular fracture mode. Whereas the fatigue crack growth behavior of Sn-37Pb and Sn-3.0Ag-0.5Cu solders tested under frequencies of 1 and 0.1 Hz at 70°C and 0.1 Hz at room temperature were predominantly time-dependent with intergranular fracture mode.

2. Fracture surface of Sn-37Pb solder showed intergranular fracture with small dimples in time-dependent region. On the other hand, that of Sn-3.0Ag-0.5Cu solder also showed intergranular fracture but with large dimples.

5. References

[1] Kariya, Y. and Suga, T. (2006). Low-cycle fatigue properties of eutectic solders at high temperatures, *Fatigue & Fracture of Engineering*

Materials & Structures, Vol. 30, August 2006, pp. 413-419.

[2] Kanchanomai, C., Miyashita, Y. and MUTOH, Y. (2001). Low-cycle fatigue behavior and mechanisms of a lead-free solder 96.5Sn/3.5Ag, *Journal of electronic materials*, Vol. 31(2). October 2001, pp. 142-151.

[3] Yu, J., Joo, D.K. and Shin, S.W. (2002). Rupture time analyses of the Sn-3.5Ag solder alloys containing Cu or Bi, *Acta Materialia*, May 2002, Vol. 50, pp. 4315-4324.

[4] Solomon H.D., Life prediction and accelerated testing. In: D.R. Frear, S.N. Burchett, H.S. Morgen, J.H. Lau, editors. The mechanics of solder alloy interconnects, New York: Van Nostrand Reinhold, (1994) 199-313.

[5] Xie, D.J., Chan Y.C., LA, J.K.L. and Hui, I.K. (1996). Fatigue lift estimation of surface mount solder joints, *IEEE Transactions on components, packaging, and manufacturing technology*, August 1996, Vol.19 (3), pp. 669-678.

[6] Zhao, J., Miyashita, Y., and Mutoh, Y. (2001). Fatigue crack growth behavior of 96.5Sn-3.5Ag lead-free solder, *International Journal of Fatigue*, February 2001, Vol. 23, pp. 723-731.

[7] Zhao, J., Mutoh, Y., Miyashita, Y. and Wang, L. (2002). Fatigue crack growth behavior of Sn-Pb and Sn-based lead-free solders, *Engineering fracture Mechanics*, October 2002, Vol. 70, pp. 2187–2197.

[8] JSMS Committee on High Temperature Strength of Materials, (2000), Low Cycle Fatigue Standard for Solder Testing, Japan Society of Material Science.

[9] Dowling, N.E. (1976). Geometry effect and J integral approach to elastic-plastic fatigue crack growth, *ASTM STP 590*, Mechanics of crack growth, Edited by Rice, J.R. and Paris, P.C, pp.82-103.

[10] Yafuso, T., Itokazu, M., Kacou, T.A.P., Kubo, S. and Ohji, K. (1995). Evaluation of the J-Integral range of fatigue crack emanating from notches by simple estimation formulae, *JSME international journal*, *Mechanics and material engineering*, Vol. 38 (1), pp. 97-103.

[11] Kanchanomai, C. and Mutoh, Y. (2008). Time-dependent fracture mechanics approach to crack growth of solder, *Journal solid mechanics and materials engineering*, July 2008, Vol. 2(10), pp. 1318-1329.

[12] Yoda, M., Nabetani, M. and Okabe, H. (2002). Creep crack growth characteristics of polypropylene film at various temperatures, *Engineering Fracture Mechanics*, February 2003, Vol. 70, pp. 2235-2246.

[13] ASTM standard test method for measurements of fatigue crack growth rates (E647-93). Annual Book of ASTM Standards 0301, (2008), American Society for Testing and Materials.

[14] Lin, C.K., and Teng, H.Y. (2006). Creep properties of Sn-3.5Ag-0.5Cu lead-free solder under step-loading, *Journal of Materials Science*, March 2006, Vol. 17, pp. 577-586.

[15] Sundelin, J.J., Nurmib, S.T. and Lepist, T.K. (2007). Recrystallization behaviour of SnAgCu solder joints, *Materials Science and Engineering A*, April 2007, Vol. 474, pp. 201-207.